TEMPORAL AND AMPLITUDE CHARACTERISTICS OF OPTICAL PULSED RADIATION TRANSMITTED THROUGH A CLOUDY LAYER

V.A. Korshunov

Scientific-Production Company "Taifun",
USSR State Committee for Hydrometeorology, Obninsk
Received December 15, 1989

The Monte Carlo method has been used to obtain the temporal and amplitude characteristics (TAC) of pulsed radiation transmitted through a cloudy layer in the case of perpendicular incidence of a wide unidirectional beam. TAC for the radiation intensity as a function of the angle of observation and for the radiation power with different angles of reception for optical thicknesses $\tau \le 50$ are obtained. The character of these dependences is mainly determined by the presence of two components of radiation — diffuse and small-angle, which have different temporal scales and angular dependences.

When optical pulsed radiation propagates in a cloudy medium its scattering and absorption by the particles of the medium result in a distortion of the pulse envelope and change in its temporal-amplitude characteristics (TAC). Quite a few papers are devoted to an' investigation of this problem, the results of which are presented, for example, in Refs. 1–3. However, a complete picture of the effect of the scattering medium on the TAC of pulsed radiation has not been yet developed. Only the cases of extremely large and relatively small (the small-angle approximation) optical thicknesses of the medium have been studied with the help of approximate methods for solving the transfer equation. With the small-angle approximation some assumptions about the scattering phase function and the angular dependence of the radiation intensity in the medium[3] are usually introduced, the effect of which on the results is difficult to evaluate. Therefore, numerical simulation by the Monte Carlo method[1] must be used together with the development of approximate methods.[4] A number of prior results obtained by the Monte Carlo method pertain to the particular case of recording the irradiance when the detector is placed on the boundary of the medium.[2,5]

In this paper an analysis of the TAC for pulsed radiation transmitted through a cloudy layer, as a' function of the angle of observation and field of view of the receiver, was performed using the Monte Carlo method. The case of perpendicular incidence of a wide unidirectional beam is considered. In fact, this corresponds, for example, to an experimental setup in which a radiation source of small dimensions is situated above a cloudy layer quite far from its upper boundary and the receiver is located on the Earth's surface. The temporal dependences of the intensity $I(u)$ were calculated (where $u = \sigma ct$ is dimensionless time, σ is the attenuation coefficient of the cloudy medium, c is the velocity of light, and t Is the time for observations made at am angle φ with respect to the normal to the layer and also of the power $P(u)$, which was recorded with the help of the receiver with the field-of-view angle $2\varphi_r$ located at a distance R_0 from the boundary of the layer (or $\tau_0 = R_0\,\sigma$ in dimensionless units) with its optical axis perpendicular to the layer boundary.

The time u was reckoned from the moment of arrival of the direct beam at the point where the receiver was located. The calculations were performed for the scattering phase function corresponding to the Deirmendjian C-1 cloud model[7] at the wavelength $\lambda = 0.45$ µm. The probability of survival of the photon was assumed to be equal to 1.

The following TAC for the pulsed radiation were chosen for analysis: the maximum value (the amplitude of the pulses I_m and P_m), the pulse duration at half maximum $\Delta_{0.5}$, and the rms width $\delta_r = \sqrt{\overline{u^2} - \overline{u}^2}$. An estimate of the pulsewidth at some level with respect to the maximum (in this case the 0.5 level was taken) is widely used in experimental research. The value δ_r appears quite often in approximate techniques as an estimate of the pulsewidth.[3]

In the solution of this problem it is necessary to take account of a peculiarity in the intensity of the scattered radiation $I_s(u)$ for $\varphi = 0$ as $u-$ 0 (Ref. 8) which takes place when the temporal behavior of the source can be characterized by a δ-function. The results obtained in Ref. 8 show that the above-mentioned peculiarity results in the logarithmic spreading of the power of the scattered radiation $P_s(u)$ as $u-$ 0, hence, the amplitudes I_{sm} and P_{sm} for $\varphi = 0$ have a finite value only when the initial pulse has a finite width. At the same time, for $\varphi \ne 0$ the value I_{sm} remains finite even for an initial δ-function pulse. In the stationary case the peculiarity in the intensity for $\varphi = 0$ is absent.

0235-6880/90/11 1047-5 $02.00

Taking into account the above-mentioned fact, we obtained a value of P_m for a pulse of finite width incident on the medium. In this paper as well as in Ref. 1 the envelope of the initial pulse is assumed to be described by the function

$$f_\kappa(u) = \kappa^2 u \exp(-\kappa u). \quad (1)$$

The initial pulsewidth at half maximum described by Eq. (1) is $\delta_\kappa = 2.447\kappa^{-1}$. For the widely used *Q*-switched laser sources the value δ_κ lies in the range of 0.1–0.5 If we take the values of σ typical for stratified clouds in calculating the dimensionless time.

In the Monte Carlo calculations $P(u)$ was determined for $\varphi_d \geq 5°$ by the direct simulation method for the propagating radiation. To determine $P(u)$ for $\varphi < 5°$ and to find $I(u)$ for any φ the local estimate (for angular variables) was employed. The maiximum number of trajectories which were averaged was $\sim 5 \cdot 10^5$. The error in the estimate of the amplitude parameters did not exceed 15% while for the temporal parameters it was ≤ 30%.

Let us now analyze the calculated results. Figure 1 shows the dependence of the intensity $I(u)$ for the observation angle $\varphi = 5°$ for $\tau = 4$, 10, 15, 20, and 25 (solid curves 1–5). It can be seen from Fig. 1 that the dependence $I(u)$ for $\tau \geq 15$ takes on a bimodal character. In addition, the first mode is formed with rather small ($u < 0.1$) time delays as compared with τ. For $\tau \leq 10$ the second mode is not formed, however, a delayed decay of the intensity (following approximately a power-law function) the tail of the pulse is observed for $0.05 < u < 1$.

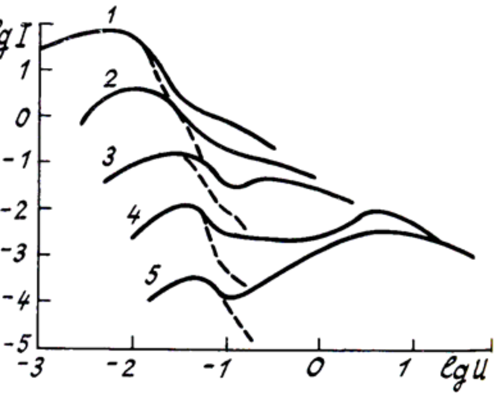

FIG. 1. Temporal behavior of the intensity I of the radiation transmitted through the cloudy layer.

To clarify the nature of the bimodal temporal structure, test calculations of the scattering phase function truncated at some sufficiently small scattering angle γ_g were performed. In this case in the numerical simulation the photon trajectory was broken off when scattering occurred at an angle $\gamma > \gamma_g$. The calculations for $\gamma_g = 10°$ are shown in Fig. 1 (dashed lines). This figure shows that for the truncated scattering phase function only the first maximum is reproduced, after which $I(u)$ drops sharply. Hence, the first maximum is caused only by small-angle scattering. In the formation of the second maximum all the scattering angles contribute. Two components of the scattering field, namely, the small-angle and diffuse, correspond to these two maxima. With increase of τ the value of the temporal shift of the maxima of these two components increases at a different rate, which results in their separation in time and the formation of the bimodal temporal structure.

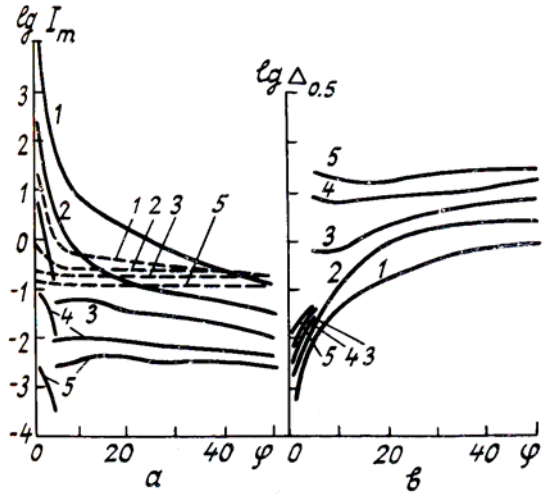

FIG. 2. The amplitude I_m (a) and the pulse width $\Delta_{0.5}$ (b) versus the angle of observation φ.

Figure 2 shows the TAC as a function of angle for the pulses with intensity $I(u)$ for different values of τ (the values τ are identical to those in Fig. 1). For comparison, the dependence of the intensity for the stationary radiation (dashed lines) is also plotted in Fig. 2a.

One can see from Fig. 2 that for small $\tau \leq 10$ there exists a well-pronounced angular dependence of the quantities I_m and $\Delta_{0.5}$: they change by several orders of magnitude as φ increases from 1 to 50*. This is associated with the strong anisotropy of the scattering phase function of the cloud.

For $\tau \geq 15$ the character of the angular dependence changes as a result of the appearance of the bimodal structure of the pulses. In addition, calculations show that for sufficiently small φ the amplitude of the first maximum is greater than in the second case and the angular dependence of the TAC is determined by the small-angle component. As for larger values of φ, the angular dependence of the TAC is determined by the diffuse component. In accordance with this, Fig. 2 shows the TAC of the first mode for $\varphi \leq 5°$ and TAC of the second mode for $\varphi \geq 5°$. The jump corresponds to the transition from the first to the second mode at $\varphi = 5$*.

As can be seen from Fig. 2,' the smooth dependence of $I_m(\varphi)$ corresponds to the diffuse component. The small-angle peak stands out against the background of this dependence. Its magnitude decreases as τ increases at $\tau = 25$ it becomes comparable to I_m because of the diffuse component. The analogous peak is also fixed for stationary radiation (dashed lines), however, it disappears already at $\tau = 15$.

The angular dependence of the temporal characteristic $\Delta_{0.5}$ (Fig. 2b) is also different for the small-angle and diffuse components. The discontinues increase in $\Delta_{0.5}$ by several orders of magnitude in a narrow angle (φ) interval in the transition from the small-angle to the diffuse component of the scattered field should be noted.

Let us now turn our attention to the shape of the pulses $P(u)$ observed a finite angle of reception. The characteristic feature of the shape of the pulses $P(u)$ as well as of the pulses $I(u)$ is the existence of two maxima observed for sufficiently small φ_r in the interval $10 < \tau \le 25$. Figure 3 plots the dependence of $P(u)$ at $\tau = 20$ and $\varphi_d = 2.5°$ (curves 1 and 1′), 5° (2 and 2′),10° (3), 20° (4), and 90° (5). The error in the estimate of $P(u)$ in the region of the maxima does not exceed 15%, and in the region of minima it is ≤ 30%. Curves 1–5 correspond to $\delta_\kappa = 0.2$, and 1′ and 2′ to $\delta_\kappa = 0.01$. Figure 3 shows that the bimodal temporal dependence appears when $\varphi_d = 2.5°$, 5°, and 10°. The position of the first mode and the ratio of the amplitudes of the two modes for a given value of φ_r are determined by the value δ_κ. As follows from Fig. 3, the amplitude of the first mode drops as δ_κ increases and the distance between the modes diminishes, finally resulting in the disappearance of the bimodal structure.

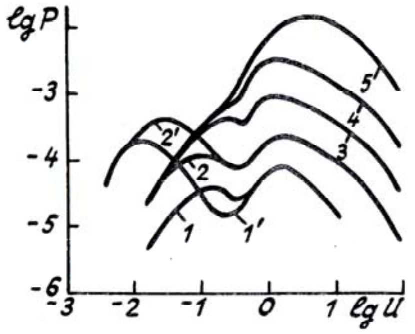

FIG. 3. Temporal behavior of the radiation power P transmitted through the cloudy layer.

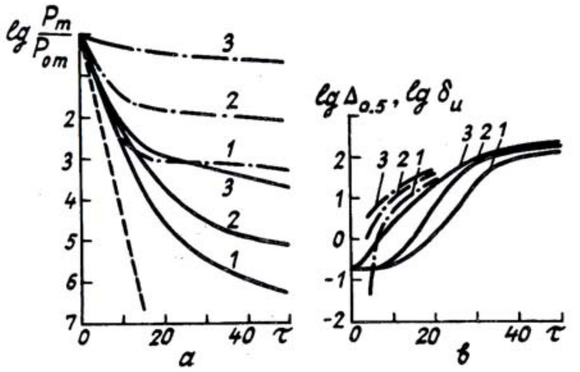

FIG. 4. Dependence *of the amplitude (a) and the temporal (b) characteristics of the power P(u) of the pulse on the optical thickness τ of the layer.*

Figure 4 plots the TAC versus τ. Figure 4a plots the ratio P_m/P_{om}, where P_{om} is the amplitude of the incident pulse. The solid lines are for $\delta_\kappa = 0.2$ and correspond to $\varphi_d = 2.5°(1)$, $10°(2)$, and $90°(3)$. The parameter τ_0 is equal to 33.33. The dot-dash lines represent the dependence of the ratio P/P_0 for the stationary case. The dashed straight line is given for comparison and corresponds to the variation of P_m/P_{om} according to the Bouguer law $\exp(-\tau)$. It follows from Fig. 4a that for small values of $\varphi_d = 2.5°$ and 10° the plotted curves have two regions which differ by the slope of the curves. The transition from one region to the other occurs for $\tau = 15$–20 for initial pulses with $\delta_\kappa = 0.2$ and $\tau = 10$–15 for the stationary case as well. In the first region of the curve, where the small-angle component predominates in accordance with the above-mentioned behavior, the variation of P_m is approximately exponential although the exponential coefficient is less than in the Bouguer law. In the second region the diffuse component predominates and the decay of P_m versus τ is delayed.

From Fig. 4a it can be seen that the attenuation of the amplitude of a pulsed signal takes place faster in comparison with the power In the stationary case. In addition, the pulse energy is obviously diminished, analogous to the power for the stationary case. Additional decrease of the amplitude is associated with temporal blooming of the pulse.

The behavior of the temporal parameters versus τ is plotted in Fig. 4b. The solid lines correspond to the same values of the parameters as in Fig. 4a. These lines show the variation of $\Delta_{0.5}(\tau)$. The dot-dash lines correspond to the rms width δ_1 for $\delta_\kappa = 0$ (in general case $\bar{\delta}_1 = \sqrt{\delta_1^2 + 0.334\delta_\kappa^2}$). Figure 4b shows that as τ increases, $\Delta_{0.5}$ at first remains constant ($\Delta_{0.5} = \text{const} = \delta_\kappa$). The constancy of $\Delta_{0.5}$ is attributed to the fact that for small τ the additional blooming of the pulse is small compared to δ_κ. After that the value of $\Delta_{0.5}$ increases sharply with τ. Here the bimodal structure exists and the value of $\Delta_{0.5}$ is taken for the mode whose amplitude is greater. From here on the diffuse component predominates and the rate of growth of $\Delta_{0.5}$ is slowed down.

The rms width δ_1, as Fig. 4(b) shows, sustantially exceeds the value of $\Delta_{0.5}$ in that region of τ where the amplitude of the pulses is determined by the small-angle component. Analysis shows that this fact can be attributed to the existence of slowly decreasing tail which increases the value of u^2 and, correspondingly, δ_1, but does not affect the value of $\Delta_{0.5}$. This fact must be taken into account when approximate methods are employed. In these methods the estimate of the pulse width is based on the temporal moments[3] of the pulse. In the region of diffuse propagation at $\tau \ge 30$ the values of the widths δ_1 and $\Delta_{0.5}$, the calculations show, become close in value.

Conclusions. The calculations performed for a wide unidirectional incident beam in the region $0 < \tau < 50$ for the observation angles $\varphi \ge 1°$ reveal a rather complicated picture of the transformation of the temporal-amplitude characteristics of pulses transmitted through a cloudy layer with the change of τ and the observation angle φ (or the reception angle $2\varphi_d$). This can be explained by the existence of two components of the scattered radiation — a small-angle component and a diffuse component, which have different time scales and angular structure (the two-scale nature of the temporal structure was noted earlier[8]).

The small-angle peak existing up to $\tau = 25$ in the region $\varphi \geq 1$ becomes pronounced against the background of the smooth dependence of the intensity of the diffuse component. At the same time, this peak disappears under the condition of a stationary radiation already prior to $\tau = 15$.

The amplitude of the pulses and their shapes in the vicinity of the maximum during recording with a finite reception angle $2\varphi_r$ are determined by the small-angle component while the second temporal moment is determined by the diffuse component.

Within the transient region $\tau = 15$–25 both components are present simultaneously and yield the bimodal pulse shape when the reception angles $\varphi_r < 10$. If $\tau > 25$ the TAC of the pulses are determined by the diffuse component.

REFERENCES

1. G.I. Marchuk et al., *The Monte Carlo Methods in Atmospheric Optics* (Springer, Berlin, 1980).
2. E.M. Feĭgel'son and L.D. Krasnokutskaya, *Fluxes of Solar Radiation and Clouds* (Gidrometeoizdat, Leningrad, 1978), 157 pp.
3. E.P. Zege, A.P. Ivanov, and I.L. Katsev, *Image Transfer in a Scattering Medium* (Nauka Tekhn., Minsk, 1985), 327 pp.
4. E.P. Zege, I.L. Katsev, and I.I. Polonskiĭ, Opt. Atm. **1**, No. 11, 19–27 (1988).
5. E.A. Bucher, Appl. Opt. **12**, No. 10, 2391–2400 (1973).
6. E.V. Genin, G.P. Kokhanenko, V.A. Krutikov, and D.S. Meshzevoi, in: *Proceedings of the 4th All-Union Conference on Propagation of Laser Radiation in a Dispersed Medium,* Part I, 83–84 Obninsk-Barnaul (1988).
7. D. Deirmendjian, *Electromagnetic Scattering on Spherical Polydispersions*, Elsevier, -Amsterdam; American Elsevier, New York (1969).
8. L.M. Romanova, Izv. Akad. Nauk, FAO **1**, No. 10, 1022–1038 (1965).